Sintering of alumina ceramics reinforced with a bioactive glass of $3CaO.P_2O_5$-SiO_2-MgO system

(Sinterização da alumina reforçada com um vidro bioativo do sistema $3CaO.P_2O_5$-SiO_2-MgO)

A. W. Huang[1], C. Santos[2,3], R. O. Magnago[2,3], R. F. F. Silva[4], K. Strecker[5], J. K. M. F. Daguano[1]

[1]Escola de Engenharia de Lorena - EEL, Universidade de S. Paulo - USPL, Polo Urbo Industrial Gleba AI-6, s/n, Lorena, SP, Brasil

[2]Faculdade de Tecnologia,UERJ - FAT, Universidade do Estado do Rio de Janeiro, Polo Industrial, km 298, Resende, RJ, Brasil

[3]Centro Universitário de Volta Redonda, UniFOA, Volta Redonda, RJ, Brasil

[4]Departamento de Engenharia Cerâmica e do Vidro, Universidade de Aveiro, CECICO, Campus Universitário de Santiago, Aveiro, Portugal

[5]Universidade Federal de S. João Del Rei - UFSJ, S. João Del Rei, MG, Brasil

anawhuang@yahoo.com.br, claudinei@demar.eel.usp.br, ju_daguano@yahoo.com.br, roberto.magnago@gmail.com, rffsilva@cv.ua.pt, strecker@pesquisador.cnpq.br

Abstract

Alumina-based ceramics, Al_2O_3, exhibit a combination of properties which favor its use as biomaterial, specifically as structural dental prosthesis. Its most important properties as biomaterial are its elevated hardness, chemical stability and biocompatibility. Usually, Al_2O_3 is processed by solid-state sintering at a temperature of about 1600 °C, but it is very difficult to eliminate the porosity due to its diffusional characteristics. The objective of this work was the development and characterization of sintered Al_2O_3 ceramics, densified with a transient liquid phase formed by a bioactive $3CaO.P_2O_5$-SiO_2-MgO glass. Powder mixtures of 90 wt.% Al_2O_3 and 10 wt.% bioglass were milled, compacted and sintered at 1200 °C to 1450 °C. Comparatively, monolithic Al_2O_3 samples were sintered at 1600 °C/120 min. The sintered specimens were characterized by relative density, crystalline phases, microstructure and mechanical properties. The results indicate that the specimen sintered at 1450 °C/120 min present the best properties. Under this sintering condition, a relative density of 95% was reached, besides hardness higher than 9 GPa and fracture toughness of 6.2 $MPa.m^{1/2}$. XRD analysis indicate alumina (αAl_2O_3), whitlockite ($3CaO.P_2O_5$) and diopsite [$3(Ca,Mg)O.P_2O_5$], as crystalline phases. Comparatively, monolithic sintered Al_2O_3 samples presented 92% of relative density with 17.4 GPa and 3.8 $MPa.m^{1/2}$ of hardness and fracture toughness respectively.
Keywords: Al_2O_3, bioactive glass ceramic, sintering, characterization, mechanical properties.

Resumo

Cerâmicas à *base de alumina exibem combinações de propriedades as quais favorecem seu uso como biomaterial, com destaque para estruturas de prótese dentária. Entre as mais importantes propriedades para uso como biomaterial estão a dureza elevada, a estabilidade química e a biocompatibilidade. Normalmente, Al_2O_3 é sinterizada no estado sólido em temperaturas superiores a 1600 °C; porem, devido às suas características difusionais, há grande dificuldade em eliminar completamente a porosidade. O objetivo deste trabalho foi o desenvolvimento e a caracterização de cerâmicas de Al_2O_3 densificadas com uma fase liquida formada por um vidro bioativo do sistema $3CaO.P_2O_5$-SiO_2-MgO. Misturas de pó com 90% em peso de Al_2O_3 e 10% em peso de vidro foram preparadas, compactadas e sinterizadas entre 1200 °C e 1450 °C. Comparativamente, amostras de Al_2O_3 monolíticas foram sinterizadas a 1600 °C/120 min. As amostras foram caracterizadas por densidade relativa, fases cristalinas, microestrutura e propriedades mecânicas. Os resultados indicaram que as amostras sinterizadas a 1450 °C/120 min apresentaram as melhores propriedades, com densidade relativa de 95% além de dureza de 9 GPa e tenacidade a fratura de 6,2 $MPa.m^{1/2}$. Análises de difração de raios X indicaram alumina (α-Al_2O_3), whitlockita ($3CaO.P_2O_5$) e diopsita [$3(Ca,Mg)O.P_2O_5$], como fases cristalinas após sinterização. Comparativamente, as amostras de Al_2O_3 apresentaram 92% de densidade relativa com 17,4 GPa e 3,8 $MPa.m^{1/2}$ de dureza e tenacidade a fratura, respectivamente.*
Palavras-chave: *Al_2O_3, vidro bioativo, sinterização, caracterização, propriedades mecânicas.*

INTRODUCTION

The development of technologies to produce novel bioceramic materials has been motivated by the growing demand of dental ceramics with improved properties in substitution of metal-based materials. The use of advanced ceramics as biomaterials started in the 1970's. Since then, they have been continually improved, specifically aiming

Table I - Hardness and fracture toughness of commercial ceramic dental materials [1].
[Tabela I - Dureza e tenacidade à fratura de cerâmicas dentárias comerciais.]

Material	Hardness (GPa)	Fracture toughness ($MPa.m^{1/2}$)
High Alumina Porcelain	4.3	2.0 - 2.9
Leucite Reinforced Glass	6.5	1.0 - 2.0
Lithium disilicate, $Li_2Si_2O_5$	6.7	3.4
Glass Infiltration - In Ceram Spinel	10	2.7
Glass Infiltration - In Ceram Alumina	13	4.4 - 4.8
Glass Infiltration - In Ceram Alumina Zircon	11	6.8
Monolithic Alumina	16	3.8 - 4.5

applications in dentistry as dental restoration parts. A usual technique for obtaining dental ceramics is the infiltration of a porous matrix with a glass. However, due to varying stages of sintering and the infiltration process, the final product has a high cost and also the possibility of having defects formed during processing which may reduce the reliability. In Table I some of the mechanical properties of commercial ceramic dental materials are listed [1].

Bioglass is a bioactive glass. Bioactivity is defined as the property to form tissue on the surface of biomaterial, establishing an interface able to supporting mechanical solicitations. Three classes of ceramic materials satisfy this criterion: the bioactive glasses and glass-ceramics, calcium-phosphate ceramics and its composites, and bio inert ceramics such as Al_2O_3 and ZrO_2-Y_2O_3. Glasses and sinter additions of Si_3N_4 and ZrO_2 have been studied [2, 3]. Recently, two works have been published, investigating the liquid-phase sintering of ZrO_2 [4, 5]. Some of these bioactive glasses can be partially crystallized by heat treatment. Studies on the effect of partial crystallization of glass-ceramics intended to improve the mechanical properties, while maintaining the bioactivity have been carried out [6, 7]. Crystallization of the glass is extremely important for the improvement of the mechanical properties. It has been shown [8, 9] that bioglasses with high crystalline fractions exhibit a decrease in their biological performance, because the formation of the HCA (Hydroxy Carbonate Apatite) layer is related to the amount of existing residual glassy phase, since its formation depends on the dissolution of calcium and silicon ions in the glassy phase [10, 11]. On the other hand, the presence of crystalline phases, which exhibit a moderate/high dissolution rate, such as wollastonite ($CaSiO_3$) [12], combeite ($Na_2Ca_2Si_3O_9$) [13] and tricalcium phosphate ($Ca_3(PO_4)_2$) [14], may play a role similar to that of a glassy phase as source of calcium and silicon ions, thus maintaining the bioactivity of the material. As example of glass-ceramics that exhibit good fracture toughness and high bioactivity are the so-called glass-ceramic A-W Cerabone® [15], and Bioverit [16].

Glass-ceramics of the $3CaO.P_2O_5$-SiO_2-MgO system with different crystalline fractions have emerged as bone substitutes because of their interesting mechanical properties [17, 18], similar to those of natural bone tissue. In a previous work [17], it was shown that the phase transformations that occur in these materials during heat-treatment under different temperatures directly influence the microstructure and hence the mechanical properties. The effect of crystallization of bioglasses on the formation of HCA is still a controversial subject and for this glass system it has not been explored yet.

In this work, Al_2O_3-based ceramics containing a bioactive glass was densified at low temperature, and the properties are compared with monolithic-Al_2O_3 sintered at 1600 °C. The effects of the glass partial crystallization on the ceramic properties are investigated.

EXPERIMENTAL PROCEDURE

Processing

High-purity α-Al_2O_3, (A-1000, Almatis-USA), and a bioactive glass based on system $3CaO.P_2O_5$-SiO_2-MgO [19, 20] have been used as starting powders. A glass composition of 52.75 wt.% $Ca_3(PO_4)_2$-30wt.% SiO_2-17.25wt.% MgO was prepared from reagent-grade $Ca(H_2PO_4)_2.H_2O$ (Synth), $CaCO_3$ (Synth), SiO_2 (Fluka) and MgO (Synth). The bioactivity of this composition was studied in samples heat-treated at 1100 °C [21].

The glass was prepared according to the conventional melting method in a platinum crucible at 1600 °C/60 min. Batches of 100 g were obtained by mixing the raw materials in ethanol for 240 min, drying at 90 °C for 24 h and passing it through a sieve with openings of 32 μm for deagglomeration. Finally, the glass was cast into cylinders with 12 mm diameter in a stainless steel mould and annealed for 120 min at 700 °C (30 °C below the glass transition temperature, T_g, of this glass) and slowly cooled down to room temperature at a rate of 3 °C/min.

A powder mixture containing 90 wt.% Al_2O_3 and 10 wt.% glass powder was prepared by planetary milling at 1000 rpm for 4 h, using ethanol as vehicle, subsequent drying at 100 °C for 24 h and sieving. Cylindrical samples of 20 mm diameter were cold uniaxially pressed under 100 MPa. The samples were sintered in a $MoSi_2$ resistance furnace, at 1200 °C, 1300 °C and 1400 °C for 60 min or at 1450 °C for 120 min, at a heating and cooling rate of 10 °C/min and 8 °C/min, respectively. Similarly, samples of α-Al_2O_3 were uniaxial

pressed and sintered at 1600 ºC/120 min with heating and cooling rate of 10 ºC/min and 8 ºC/min, respectively.

Characterization

Starting powders and sintered samples were characterized by X-ray diffractometry (XRD), Shimadzu XRD6000, using Cu-k_α α radiation (λ=1.5418Å) in the 2θ range of 20 to 80°, with a step of 0.02° and 2 s of exposure time/degree. The crystalline phases were determined by comparison with the JCPDS files [19].

The non-isothermal crystallization kinetics was studied using differential scanning calorimetry DSC Netzsch-404. Glass powder was carried out in a platinum crucible at 10 °C/min from room temperature up to 1200 °C.

In addition, the thermal expansion coefficients (TEC) of the alumina and glass (ceramic) samples were determined by dilatometry, using an alumina rod dilatometer (Bahr Thermoanalyse GmbH 2000 Dil801L-1600 ºC, Germany). Samples with 8-10 mm thickness and 3 mm × 3 mm cross-section were used for dilatometry measurements. The thermal expansion coefficient of the bulk glass and Al_2O_3 was measured in air, using heating rate and cooling rate of 25 and 5 ºC/min, respectively.

The bulk density of the sintered samples was evaluated by the Archimedes method in distilled water. The relative density was calculated as the ratio between the apparent and respective theoretical density, calculated by the rule of mixture.

Starting glass powder and sintered samples were examined by scanning electron microscopy (SEM), in a Leo-1450VP microscope. The sintered samples were cut, their surfaces ground and polished with diamond paste, washed with acetone in an ultrasonic bath for 10 min, and dried at 100 ºC for 1 h. After this step, samples were thermally etched at 1200 ºC/15 min, with heating rate 30 ºC/min to reveal the grains microstructure.

Hardness and fracture toughness (K_{Ic}), were determined using a Vickers indentation method. In each sample, 10 indentations were performed and measured, under a load of 2000 gf for 30 s. The fracture toughness was calculated by measuring the relation between cracks length (*c*) and indentation length (*a*), using the relation valid for Palmqvist crack types, which present *c*/*a* relation < 3.5 [20].

RESULTS AND DISCUSSION

Glass characterization

Fig. 1 presents the X-ray diffraction patterns of the starting materials used in this work. The Al_2O_3 powder consists of the highly crystalline α-Al_2O_3 phase, while the glass exhibits a typical amorphous pattern, indicating no crystalline phase in this material. Due to the importance of the characteristics of the bioglass used as sintering aid, the bioglass has been studied in greater detail.

The crystallization of this glass at 1100 ºC was

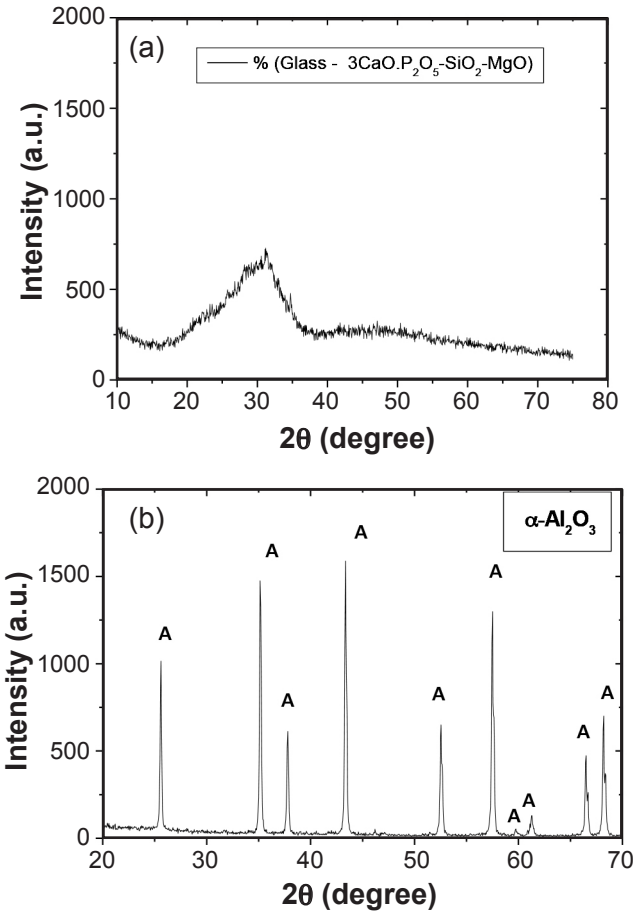

Figure 1: X-ray diffraction patterns of the bioglass and Al_2O_3 powders.
[Figura 1: Difratogramas de raios X dos pós de Al_2O_3 e biovidro.]

investigated by High Resolution X-ray Diffractometry, HRXRD, using a Hubber diffractometer with multiple axes [22]. The amount of the crystalline phases (crystallized volume fraction) contained in the glass-ceramic samples was determined according to the procedure used by Krimm and Tobolsky [23]. The percent crystallinity (IC) was calculated by the ratio of the crystalline area (AC) and the total area (AT = amorphous + crystalline), using the Origin software (OriginLab Corp., Northampton, MA) and the following equation:

$$IC = (AC / AT) \times 100 \quad (A)$$

This work confirmed the presence of crystalline phases in the material, identified as whitlockite (PDF #87-1582), a tricalcium-phosphate with magnesium in solid solution, $Ca_{2,589}Mg_{0,411}(PO_4)_2$, and is also known as the β-TCMP and diopside, $CaMgSi_2O_6$ (PDF #71-1067) [19].

The glass-ceramics studied in this work, independent on the temperature of the thermal treatment, showed whitlockite (PDF # 87-1582) as the major crystalline phase. In this phase Mg is partially substituted by Ca, forming a solid solution of $[3(Ca,Mg)O.P_2O_5]$ as will be seen below in the characterization of sintered samples.

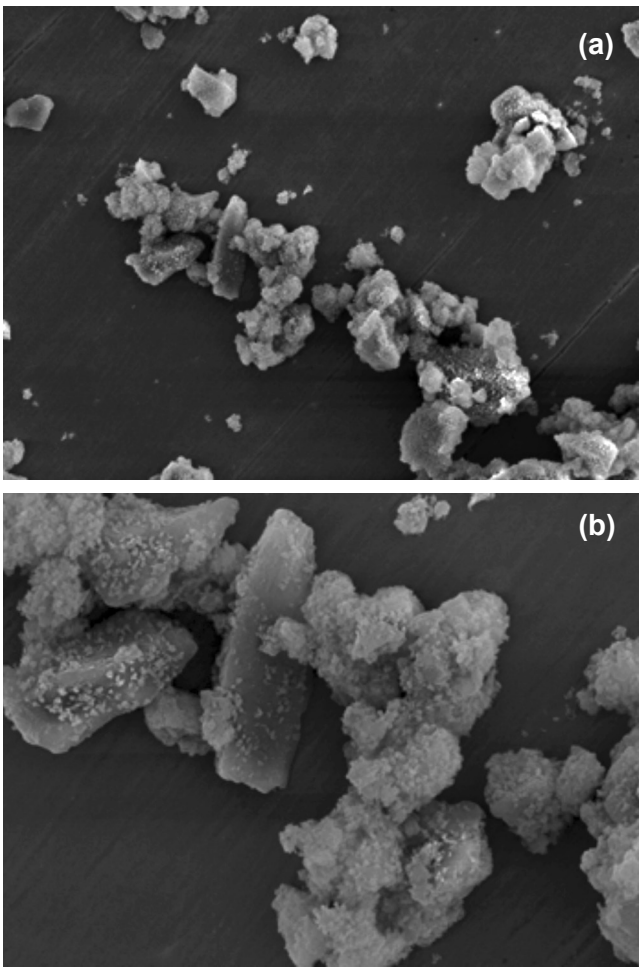

Figure 2: SEM micrographs of the bioglass particles obtained by planetary milling.
[Figura 2: Micrografias obtidas por microscopia eletrônica de varredura das partículas de biovidros obtidas por moagem em moinho planetário.]

Fig. 2 shows SEM images of the bioglass particles used as starting material. The particles are smaller than 32 μm and of irregular shape because of the crushing and milling process used in its fabrication.

The results of the Differential Scanning Calorimetry (DSC) for a monolithic sample are presented in Fig. 3. They indicate that the heat treated glass exhibits a first endothermic peak at 717 °C, which is attributed to the glass transition temperature, T_g. Two exothermic peaks were also detected at T_{p1} = 834 °C and at T_{p2} near 980 °C.

Another exothermic reaction at 1046 °C was observed in the bulk sample, but of small intensity, suggesting a phase transformation. This phase transformation could be confirmed later by the analysis of the crystalline phases. At last during cooling of the glass, an exothermic peak at T_x ~ 1115 °C was observed. Previous studies suggest that the first peak corresponds to the formation of the tricalcium phosphate with partial substitution of Mg by Ca (whitlockite) of composition 3(Ca, Mg)O.P_2O_5 and the second corresponds to the precipitation of enstatite with partial substitution of Ca by Mg, (Mg,Ca)O.SiO_2 [22]. Daguano *et al*. [21] using phase analysis by X-ray diffraction, were able to identify whitlockite and diopside as crystalline phases at 1100 °C, representing near to 70 vol.% of the samples, and the remaining 30 vol.% are in the glassy state.

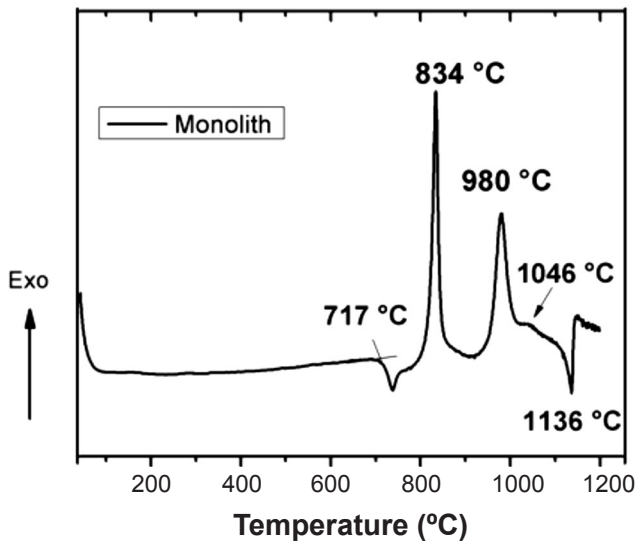

Figure 3: Thermal analysis curves of the bioactive 3CaO.P_2O_5-SiO_2-MgO glass.
[Figura 3: Curvas de análise térmica do vidro bioativo 3CaO.P_2O_5-SiO_2-MgO.]

Characterization of the sintered samples

Fig. 4 shows the results of the relative density as a function of sintering temperature. An increase of relative density is observed as function of sintering temperature. Samples sintered at 1450 °C/120 min lead to 94.5% of theoretical density. Furthermore, comparatively, monolithic samples sintered 1600 °C/120 min present relative density near to 92%. The X-ray diffraction patterns of the sintered Al_2O_3-bioglass samples are shown in Fig. 5.

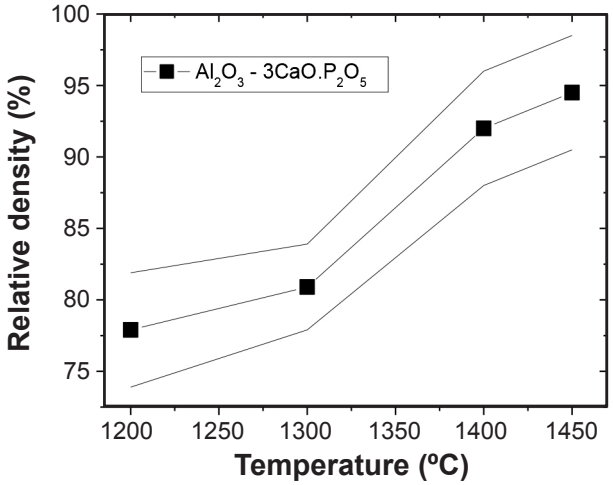

Figure 4: Relative density as a function of sintering temperature.
[Figura 4: Densidade relativa como função da temperatura de sinterização.]

The peaks of the α-Al_2O_3 phase remain unaltered, independent on the sintering temperature, and show the same positions and relative intensities as the starting powder, see Fig. 2. Besides α-Al_2O_3, the phases whitlockite [3CaO.P_2O_5] and diopsite [3(Ca,Mg)O.P_2O_5], can be observed in all sintered samples. This observation is consistent with the results of the thermal analysis of the glass, Fig. 3, which indicates the crystallization of these phases. The microstructures of the sintered samples are shown in Fig. 6.

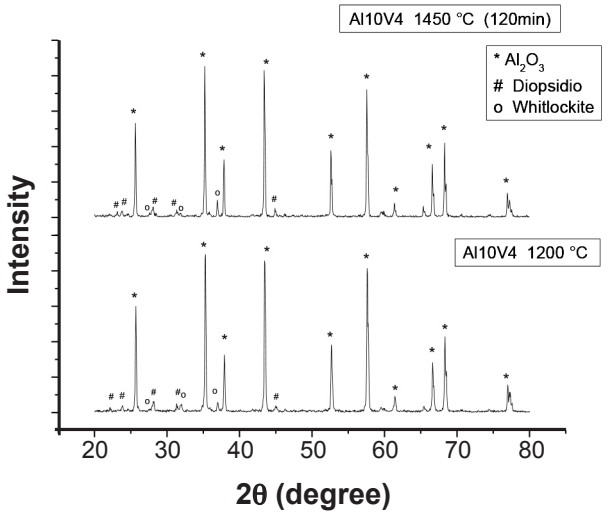

Figure 5: X-ray diffraction patterns of the Al_2O_3-glass composite ceramic sintered at 1200 ºC/60 min and 1450 ºC/120 min.
[Figura 5: Difratogramas de raios X do compósito Al_2O_3-vitrocerâmico, sinterizado a 1200 ºC/60 min e 1450 ºC/120 min.]

With increasing sintering temperature, the pore size decreases, especially when sintered at 1400 ºC or 1450 ºC. The pore sizes decrease from approximately 15 μm when sintered at 1200 ºC/60 min to less than 8 μm when sintered at 1450 ºC/120 min. These observations are consistent with the results of the final relative densities shown in Fig. 4, indicating a significant increase at relative density in the samples when sintered at 1400 ºC or 1450 ºC. These results are attributed to a decrease of the viscosity of the reminiscent glassy phase at temperatures above 1400 ºC, enhancing the liquid phase sintering mechanism [24].

Mechanical properties

The hardness and toughness of samples sintered at different temperatures are shown in Table II.

Both hardness and fracture toughness of the samples increase significantly when sintered at temperatures higher than 1400 ºC. This improvement is directly related to the

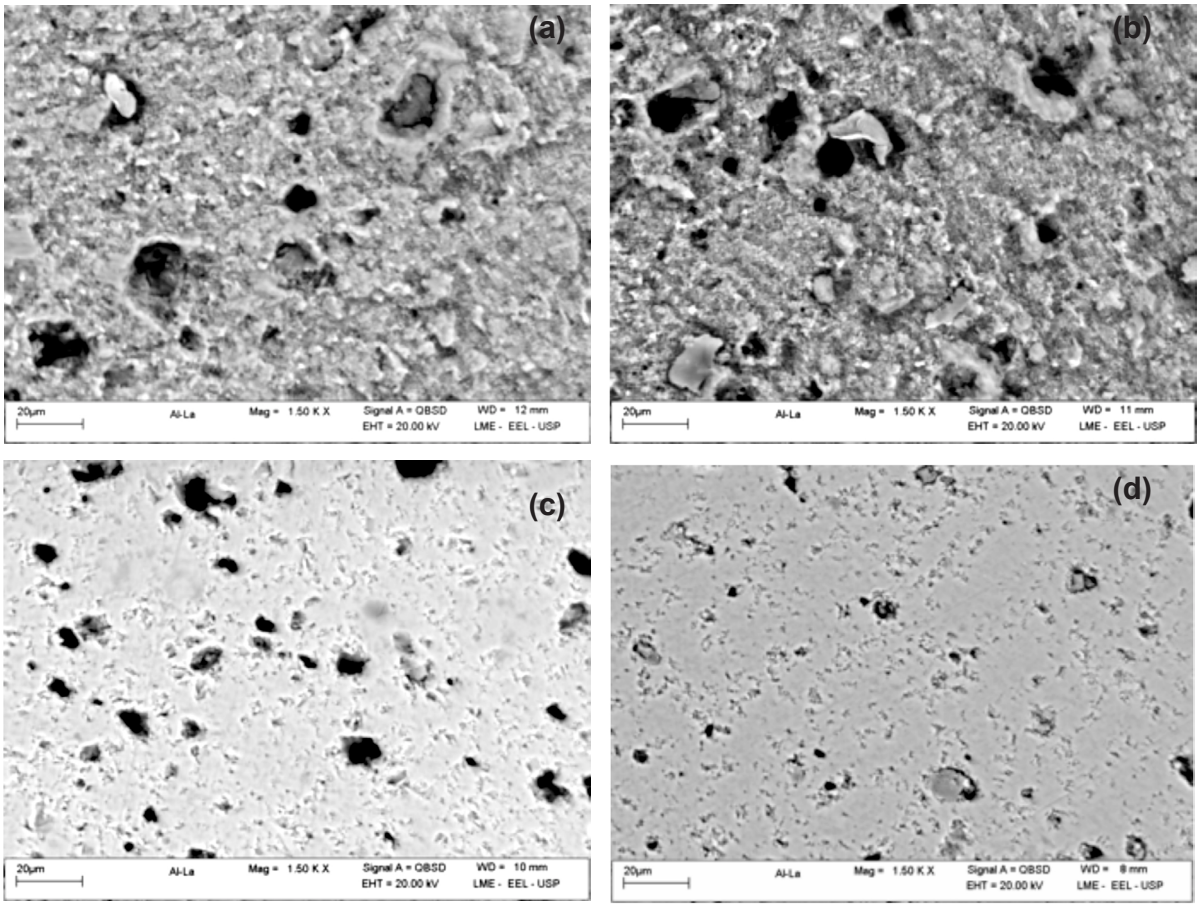

Figure 6: SEM micrographs of the sintered samples at temperatures of (a) 1200 ºC; (b) 1300 ºC; (c) 1400 ºC and (d) 1450 ºC.
[Figura 6: Micrografias em MEV de amostras sinterizadas a: (a) 1200 ºC; (b) 1300 ºC; (c) 1400 ºC e (d) 1450 ºC.]

Table II - Hardness and fracture toughness of the samples as function of sintering conditions.
[Tabela II - Dureza e tenacidade a fratura em função das condições de sinterização.]

Samples	Sintering conditions	Relative density (%TD)	Vickers hardness HV_{2000gF} (GPa)	Fracture toughness ($MPa.m^{1/2}$)
Al_2O_3-glass ceramic composite (90:10)	1200 ºC -1 h	77.9 ± 3.8	1.2 ±0.3	0.4 ± 0.3
	1300 ºC -1 h	80.9 ± 3.2	1.4 ±0.2	2.3 ± 0.2
	1400 ºC -1 h	92.0 ± 4.1	8.0 ± 0.5	5.7 ± 0.3
	1450 ºC -2 h	94.5 ± 4.2	9.0±0.5	5.9 ± 0.4
Monolithic Al_2O_3	1600 ºC -2 h	92.1 ± 3.7	17.4 ± 0.4	3.8 ± 0.5

increase of the relative density. For sintering temperatures higher than 1400 ºC, relative density higher than 90% and the hardness exceeds 8 GPa, while the fracture toughness ranges in the order of 6 $MPa.m^{1/2}$. In comparison, conventionally solid-state sintered Al_2O_3 at 1600 ºC exhibit hardness near to 17 GPa, relative density of 92% and fracture toughness 3.8 $MPa.m^{1/2}$. In applications of ceramic materials as structural components in prosthesis, lower hardness and high fracture toughness are important because they permit the preparation and restoration of parts with complex geometry, which must be machined to high quality finishing. Besides, high fracture toughness materials have also improved strength and reliability. A brief comparison with the materials properties presented in Table I permits to state that the Al_2O_3-bioglass material has good fracture toughness and similar hardness.

Theoretical residual stress

Table III shows the coefficient of thermal expansion and Young modulus of the Al_2O_3 and glass-ceramic composite phases. Previous studies [19, 23] found that these ceramics present, after heat treatment at 1100 °C, Young modulus 130 GPa with porosity 5% and 70% crystalline phase.

Table III - Coefficient of thermal expansion and Young's modulus of the Al_2O_3 and glass.
[Tabela III - Coeficiente de expansão térmica e modulo de elasticidade da Al_2O_3 e do vidro.]

Material	Coefficient of thermal expansion (CTE) $\alpha_{(25\ ºC-800\ ºC)}$	Young modulus (GPa)
$3CaO.P_2O_5$-SiO_2 glass	10.2 x 10^{-6}/ºC	130
Al_2O_3	7.5 x 10^{-6}/ºC	450

The calculation of the average thermal residual stress, generated during cooling of the sintered samples, is based on the homogeneous distribution of the second phase in the ceramic matrix, and it is directly related to the thermal expansion coefficient difference between Al_2O_3-matrix and the glassy (intergranular) phase [25-27]. This average thermal residual stress in both phases can also be calculated as a function of the volume fraction of sintering additive, following the approach using equation B and C [25].

$$\sigma_g = E_g (\langle\alpha\rangle - \alpha_g)\Delta T \quad (B)$$

$$\sigma_m E_m (\langle\alpha\rangle - \alpha_m)\Delta T \quad (C)$$

Here, σ_g and σ_m are residual stresses in the system (glass and substrate matrix, respectively). E_m and E_g indicate the Young modulus of the matrix and glass, respectively, and α_m and α_g indicate the average thermal expansion coefficient of the composite, matrix and glassy phase, respectively. The average thermal expansion coefficient for each composition can be calculated using equation D:

$$\langle\alpha\rangle = \frac{\alpha_g C_g E_g + \alpha_m C_m E_m}{C_g E_g + C_m E_m} \quad (D)$$

where C_g and C_m are, respectively, the fraction of glass and matrix. Based on the above calculation, one finds that, on average, when $\alpha_m > \alpha_g$ and $\sigma_g < 0$, the grain boundary will be in compression and the matrix will be in tension [25, 26]. Residual stress in multiphase composites develops due to the mismatch of the E-modulus and the thermal expansion coefficient in the constituent phases. Due to the lower TEC of the glass α_b than that of the matrix α_m, residual tensile stresses are developed in the Al_2O_3-glass ceramic matrix

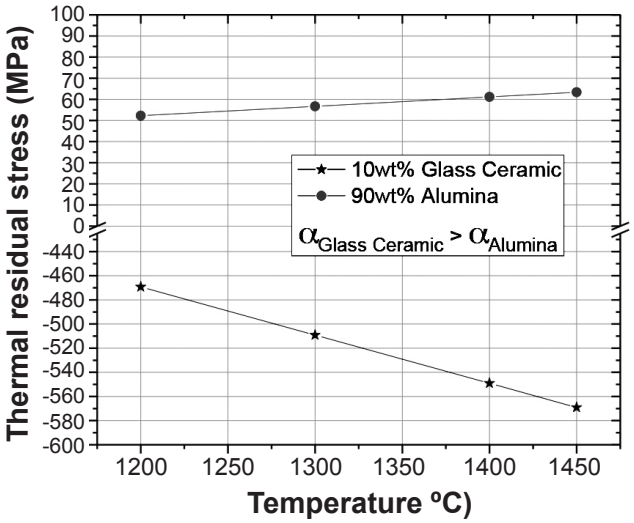

Figure 7: Theoretical residual stress as function of sintering temperature.
[Figura 7: Tensão residual teórica como função da temperatura de sinterização.]

during cooling. The residual stress in the multiphase composites is developed because of the mismatch in the E-modulus and the thermal expansion coefficient among the constituent phases. Fig. 7 shows the theoretical residual stress of the composite and indicates a tensile stress in order of 500 MPa in the glass-ceramic phase, which promotes the crack deflection and the formation of grains bridging.

CONCLUSIONS

This work shows that it is possible to sinter alumina ceramics by liquid phase sintering, using bioglass as additive, at lower temperatures as compared with conventional solid-state sintered alumina. Adding 10 wt.% of bioglass as sintering aid to Al_2O_3, a relative final density of 95% could be achieved at temperatures as low as 1450 ºC, with a hardness of ~ 9G Pa and a fracture toughness of 6.5 MPa.$m^{1/2}$. Furthermore, a partial crystallization of the intergranular glassy phase into 3(Ca,Mg)O.P_2O_5, whitlockite, and (Mg,Ca) O.SiO_2, enstatite, has been observed and that inhibited the full densification of these ceramics. The comparison with monolithic α-Al_2O_3 sintered at 1600 ºC/120 min indicates an increasing of 2.6% in relative density and 54% in fracture toughness, while the hardness was reduced to ~ 48% relative to monolithic Al_2O_3.

ACKNOWLEDGMENTS

The authors would like to thank the Brazilian research funding agency FAPESP (Fundação de Amparo à Pesquisa do Estado de S. Paulo) for financial support (Grants 04/04386-1 and 06/50510-1).

REFERENCES

[1] K. J. Anusavice, Phillips - Materiais dentários, 11nd Ed. Elsevier (2005).
[2] M. Amaral, M. A. Lopes, R. F. Silva, J. D. Santos, "Densification route of Si_3N_4 - bioglass biocomposites", Biomaterials **23**, 3 (2002) 857-862.
[3] T. H. Huang, P. F. James, "A New Machinable Phosphate Based Glass-Ceramics", in Conference Warwick University, April (1990).
[4] C. Santos, R. C. Souza, N. Almeida, F. A. Almeida, R. R. F. Silva, M. H. F. V. Fernandes, "Toughened ZrO_2 ceramics sintered with a La_2O_3-rich glass as additive", J. Mater. Proc. Techn. **200**, 1-3 (2008) 126-132.
[5] C. Santos, R. C. Souza, A. F. Habibe, L. D. Maeda, "Mechanical properties of Y-TPZ ceramics obtined by liquid phase sintering using bioglass as additive", Mater. Sci. Eng. A **478**, 1-2 (2008) 257-263.
[6] D. C. Clupper, L. L. Hench, J. J. Mecholsky, "Strength and toughness of tape cast bioactive glass 45S5 following heat-treatment", J. Eur. Ceram. Soc. **24** (2004) 2929-34.
[7] S. Bhakta, D. K. Pattanayak, H. Takadama, T. Kokubo, C. A. Miller, M. Mirsaneh, I. M. Reaney, I. Brook, R. Noort, P. V. Hatton, "Prediction of osteoconductive activity of modified potassium fluorrichterite glass-ceramics by immersion in simulated body fluid", J. Mater. Sci. Mater. Medicine doi: 10.1007/s10856-010-4145-y (2010).
[8] O. Peitl, G. P. LaTorre, L. L. Hench, "Effect of crystallization on apatite-layer formation of bioactive glass 45S5", J. Biomedical Mater. Res. **30** (1996) 509-14.
[9] T. Kokubo, "Bioactive glass-ceramics: properties and applications", Biomaterials **12** (1991) 155-63.
[10] A. Hoppe, N. S. *Güldal*, A. R. Boccaccini, "A review of the biological response to ionic dissolution products from bioactive glasses and glass-ceramics", Biomaterials **32** (2011) 2757-74.
[11] P. Li, Q. Yang, F. Zhang, "The effect of residual glassy phase in a bioactive glass-ceramic on the formation of its surface apatite layer in vitro", J. Mater. Sci. Mater. Medicine doi: 10.1007/BF00701242 (1992).
[12] M. A. Casa-Lillo, P. Velásquez, P. N. De Aza, "Influence of thermal treatment on the in vitro bioactivity of wollastonite materials", J. Mater. Sci. Mater. Medicine **22** (2011) 907-15.
[13] H. Arstila, E. Vedel, L. Hupa, M. Hupa, "Factors affecting crystallization of bioactive glasses", J. Eur Ceram Soc. **27** (2007) 1543.
[14] S. Kannan, F. Goetz-Neunhoeffer, J. Neubauer, S. Pina, P. M. C. Torres, J. M. F. Ferreira, "Synthesis and structural characterization of strontium-and magnesium-co-substituted Beta-tricalcium phosphate", Acta Biomaterialia **6** (2010) 571-76.
[15] T. Kokubo, S. Ito, S. Sakka, T. Yamamuro, "Formation of a high-strength bioactive glassceramic in the system MgO-CaO-SiO_2-P_2O_5", J. Mater. Sci. **21** (1986) 536-34.
[16] O. Peitl, E. D. Zanotto, G. P. La Torre, L .L. Hench, "Bioactive ceramics and method of preparing bioactive ceramics", Patent WO/1997/041079, November 06 (1997).
[17] J. K. M. F. Daguano, C. Santos, M. H. F. V. Fernandes, S. O. Rogero, K. Strecker, "Effect of partial crystallization on the mechanical properties and cytotoxicity of bioactive glass from the 3CaO.P_2O_5-SiO_2-MgO system", J. Mechan. Behavior Biomedical Mater. **14** (2012) 78-88.
[18] T. Kokubo, H. Takadama, "How useful is SBF in predicting in vivo bone bioactivity?", Biomaterials **27** (2006) 2907-15.
[19] Powder Diffraction File Inorganics Phases: alphabetical index, inorganics phases, JCPDS/International centre for diffraction data, Swarthmore, Pennsylvania (1979).
[20] K. Niihara, R. Moreno, D. P. H. Hasselman, "Evaluation of KIC of brittle solids by the indentation method with low crack-to-indent ratios", J. Mater. Sci. Lett. **1** (1982) 13-16.
[21] J. K .M. F. Daguano, S. O. Rogero, M. C. Crovace, O. Peitl Filho, K. Strecker, C. dos Santos, "Bioactivity and cytotoxicity of glass and glass-ceramics based on the 3CaO. P_2O_5-SiO_2-MgO system", J. Mater. Sci. Mater Medicine **24**, 9 (2013) 2171-80.
[22] J. K. M. F. Daguano, P. A. Suzuki, K. Strecker, M. H. F. V. Fernandes, C. Santos, "Evaluation of the micro-hardness and fracture toughness of amorphous and partially crystallized 3CaO.P_2O_5-SiO_2-MgO bioglasses", Mater. Sci. Eng. A **533** (2012) 26-32.

[23] S. Krimm, A. V. Tobolsky, "Quantitative X-ray studies of order in amorphous and crystalline polymers. Quantitative X-ray determination of crystallinity in polyethylene", J. Polymer Sci. **7** (1951) 57-76.
[24] W. D. Kingery, *Sintering in the presence of a liquid phase*, Editor MIT Press (1957) 235.
[25] J. L. Shi, L. Li, J. K. Guo, "Boundary stress and its effect on toughness in thin boundary layered and particulate composites: model analysis and experimental test on T-TZP based ceramic composites", J. Eur. Ceram. Soc. **18** (1998) 2035-2043.
[26] J. L. Shi, Z. L. Lu, J. K. Guo, "Model analysis of boundary residual stress and its effect on toughness in thin boundary layered yttria-stabilized tetragonal zirconia polycrystalline ceramics", J. Mater. Res. **15**, 3 (2000) 727-732.
[27] M. Taya, S. Hayashi, A. S. Kobayashi, H. S. Yoon, "Toughening of a particulate-reinforced ceramic-matrix composite by thermal residual stress", J. Am. Ceram. Soc. **73**, 5 (1990) 1382-1391.
(Rec. 06/11/2014, Ac. 06/03/2015)